Journal of Engineering Science | | Vol. XXXI, no. 4 (2024), pp. 73 - 83
Fascicle Electronics and Computer Science ISSN 2587-3474
Topic Electronics and Communication eISSN 2587-3482

https://doi.org/10.52326/jes.utm.2024.31(4).05
UDC 681.586:629.783:004.8

ARCHITECTURE OF THE SPACE RADIATION SENSOR SATELLITE MODULE BASED ON ARTIFICIAL INTELLIGENCE

Nicolae Secrieru [1]*, ORCID: 0000-0002-9168-6049,
Viorel Carbune [1], ORCID: 0000-0002-1556-4453,
Tudor Zadorojneac [1], ORCID: 0000-0002-4079-252X,
Vladimir Melnic [1], ORCID: 0000-0003-4180-3654,
Mihai Ivanovici [2], ORCID: 0000-0002-0803-2918,
Andrei Bertescu [2], ORCID: 0009-0004-7464-0075,
Stefan Popa [2], ORCID: 0000-0001-9275-4536,
Artur Kazak [2], ORCID: 0000-0002-1463-9089

[1] *Technical University of Moldova, 168, Ștefan cel Mare Blvd., Chișinau, Republic of Moldova*
[2] *Transilvania University of Brasov, Brașov, Romania*
* Corresponding author: Nicolae Secrieru, *nicolae.secrieru@cnts.utm.md*

Received: 10. 05. 2024
Accepted: 11. 12. 2024

Abstract. This paper is dedicated to the study of the cosmic radiation and its effects on electronics, as well as methods to measure it in order to aid the elaboration of the architecture of the satellite module with space radiation sensors for classification and real-time analysis of cosmic radiation-induced fault patterns and state predictions the of electronic systems embedded in satellites. The architecture of the satellite module with an intelligent radiation sensor based on an FPGA device is proposed, which will include as radiation sensing elements arrays of various types of electronic memories (on semiconductors), both within the circuit and external nearby this circuit. A significant part of the FPGA circuit configuration consists in the development of acquisition, processing and communication procedures using structures with majoritz voting to exclude the influence of spatial radiation.

Keywords: *space radiation sensor, satellite module, artificial intelligence.*

Rezumat. Această lucrare este dedicată studiului radiației cosmice și efectelor acesteia asupra electronicii, precum și modalităților de măsurare a acesteia pentru a ajuta la dezvoltarea arhitecturii modulului satelit cu senzori de radiație spațială pentru clasificarea și analiza în timp real a tiparelor de defecțiuni induse de radiația cosmică și predicția stării sistemelor electronice încorporate în sateliți. Este propusă arhitectura modulului satelit cu senzorul inteligent de radiație bazat pe un circuit de tip FPGA, care va include ca elemente de detectare a radiației rețele de diferite tipuri de memorii electronice (pe semiconductori), atât în interiorul circuitului, cât și în exteriorul apropiat al acestuia. O latură semnificativă a configurării circuitului FPGA constă în realizarea procedurilor de achiziție, procesare și comunicare utilizând structuri cu vot majoritar pentru a exclude influența radiației spațiale.

Cuvinte-cheie: *senzor de radiație spațială, modul satelit, inteligență artificială.*

1. Introduction

Space radiation poses a significant threat to the electronic components of satellites in Earth orbit and spacecrafts on planetary missions. The particles in the cosmic space are the high-energy electrons, protons, alpha particles and cosmic rays. Space radiation can lead to disruptions and temporary malfunctions in integrated circuits, including memory components. While the natural space environment does not have high level dose pulses, electronic systems exposed to space radiation can accumulate a large sum dose of electrons and protons over many years [1,2].

The radiation effects caused by high-energy particles in space are mainly determined by the ionization process, in which high level energy particles generate electron and hole pairs (e-h) as they pass through the equipment.

In complement to generating electron and hole (e-h) pairs, radiation can cause deformation damage in the atomic semiconducter lattice by breaking atomic bonds and forming so-called recombination centers and centers by accretion. Both damage mechanisms can lead to decreased electronic scattering. The X-rays and gamma rays are the main ionizing electromagnetic radiations. The ionizing radiation consists of light uncharged particles (neutrons), light charged particles (electrons, protons), alpha and beta particles and heavy charged particles (heavy ions) of chemical elements such as iron, bromine, krypton, xenon. Gamma rays and X-rays cause damage similar to that caused by light-charged particles because their main effect is the interaction of charge with the atomic structure of the material. Neutrons are uncharged and interact primarily with the atomic nuclei, causing damage in the atomic lattice of the material [1,3,4].

Therefore, the development of space radiation sensor based on artificial intelligence would give the possibility to more adequately assess the state of space weather and will give the possibility to mitigate its negative effects.

2. Space Radiation Measurement Approaches

The purpose of the research is to analyze the deviations of sensor parameters over time and as a function of the accumulated spatial radiation dose. It is known that the absorbed radiation dose refers to the amount of radiation energy delivered per unit mass of material. This is usually measured in rad (absorbed radiation dose) or in international units such as Gray or mGy (milliGray = 1/1000 Gray).

At the current stage there are a variety of methods and means of radiation measurement [1], but semiconductor based detectors are preferred due to the principle of radiation responsiveness, mass and energy consumed. The radiation reaction occurs when a particle imposes energy on a semiconductor detector or semiconductor junction, resulting in an equal number of electrons and holes being created along the particle's path within a few picoseconds. The detector is designed to ensure that an electric field is present throughout the active volume, causing the charge carriers to experience electrostatic forces that drive them in opposite directions. Therefore, the movement of these electrons and holes generates a current that continues until the carriers are collected at the boundaries of the active volume of the semiconductor material.

Taking into account the effects of radiation on semiconductors, in this paper we will focus on semiconductor-based sensors.

3. Architecture of the space radiation sensor satellite module

The architecture of a prototype satellite module is proposed with the objectives to verify the value of a demonstration mission, which are of great interest both locally and internationally: to assess the feasibility of using a radiation sensor based on artificial intelligence and realized with Commercial-off-the-shelf components. At the core of this module is a Field Programmable Gate Arrays (FPGA) device circuit [5-9], in which several Single-Event Upset (SEU) detector arrays are embedded in the silicon area/surface of the circuit. The FPGA device will be configured with a custom design aimed at detecting SEUs and then clustering and classifying the patterns using an AI model. The device will be hosted on an auxiliary printed circuit board interfaced to the Onboard Computer's (OBC) main board through a connector. The four objectives of the AI-based hardware Cosmic Radiation Sensor (AICoRS) system are: i) evaluating the feasibility of using an FPGA device as a cosmic radiation sensor, ii) measuring and classifying the cosmic radiation patterns, iii) evaluating the effectiveness of SEU mitigating mechanisms (e.g. triple modular redundancy (TMR), error correction code and iv) evaluating the feasibility of using such a modern, low-cost general-purpose FPGA device for space applications. Based on the AMD FPGA the proposed system will contain: the FPGA device, voltage regulators for ensuring the required supply voltages, total and per voltage level current monitors for measuring the power draw, low-jitter oscillators for supplying clock signals, non-volatile flash memories for storing the FPGA configuration files, the necessary voltage levels converters for the data signals between the OBC and the FPGA and ICs for control (e.g. reset, enable/disable, configuration modes). All these devices contribute to the power draw. The board should support in-space FPGA reconfigurability. More details on the composition and functioning of this core are presented in [10].

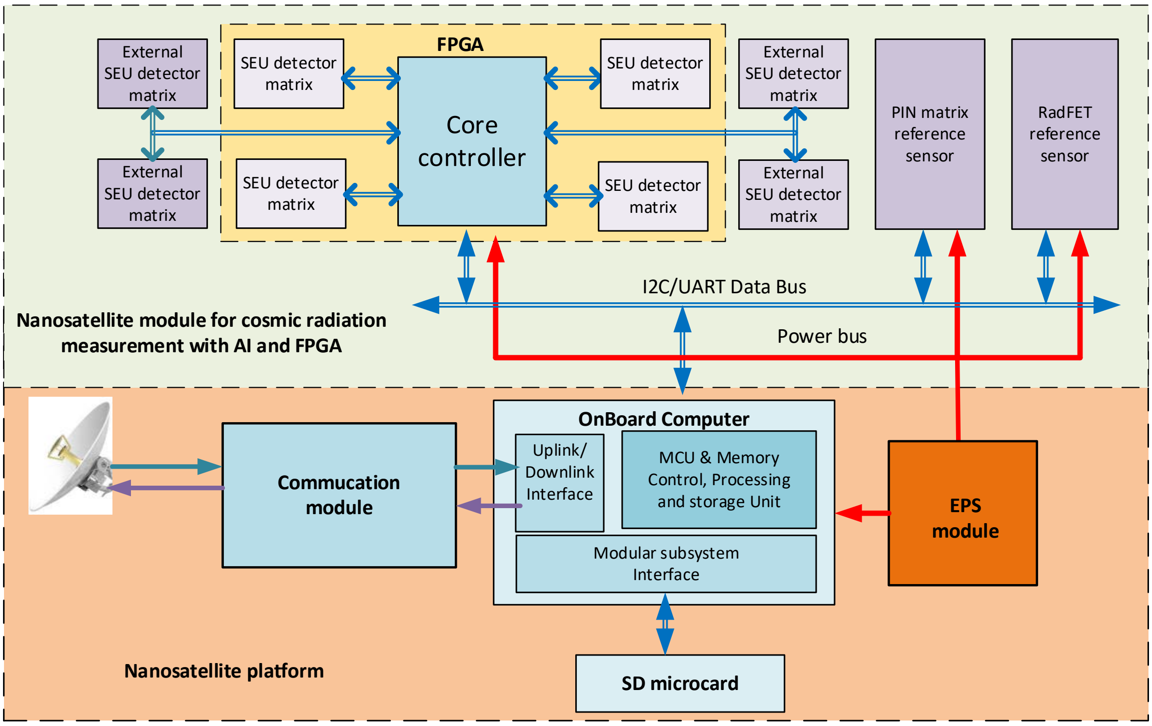

Figure 1. The functional schema of the space radiation sensor satellite module.

This core will be realized separately as a space radiation sensor with artificial intelligence properties. This satellite module has not only the technological demonstration mission, but also the test/verification mission for training the artificial neural network. For this purpose, reference radiation sensors are proposed to accumulate veridical information of the types and intensities of spatial radiation, which will be further characterized.

4. Reference Sensors External to the FPGA

In order to propose solutions for External Sensors to the FPGA and other Reference Sensors a number of dosimetry methods have been considered, but we have limited ourselves to those based on [1-4,9,11]:

- memory dosimetry - single events cause bit flips/changes in memory - the accumulated number of errors reflects the absorbed dose;
- PIN diodes - voltage change before and during irradiation;
- RadFET transistors - p-MOS transistor threshold voltage shift indicates irradiation.

Memory dosimetry. After analyzing the reaction of various types of memory to radiation, it has been found that emerging resistance-shifting memory technologies such as Magnetoresistive random-access memory, Resistive random-access memory (ReRAM), Conductive bridging random access memory (CBRAM) and Phase-change random-access memory (PCRAM) (as known under typical names) are relatively insensitive to ionizing radiation, single event effects (SEE) and displacement damage, since there is no direct relation of interaction between radiation and the storage mode. But when radiation induced errors may arise, they are most common is the result of an interaction with the decoding unit or supporting peripheral circuitry. [2,9].

Therefore, as an external SEU detection to the FPGA it is proposed nonvolatile memory (NVM) arrays, which are less tolerant, i.e., more sensitive to cosmic radiation. There memories are usually arranged in arrays that are read and written operations using orthogonal address lines (AL) and data lines (DL). However different array topologies are used for different memory device technologies. For instance, three terminal charge based devices such as embedded floating gate (EFG) or charge trapping memory (CTM) are applied in NAND and NOR flash topologies. [2-4, 9, 11]. For two-terminal resistive type memories are more often applied in the form of dynamic random access memory (DRAM-like) random access arrays, which allow separate read and write operations on discrete cells.

The operations "write" or "program", for charge based memories, indicate the injection of charge into the storage element (FG or capture layer), while "erase" usually refers to the process of removing the charge. Usually, these terms are used to indicate reading and writing to NVM-type memory, which depends on the technology discussed. The operations "set" and "reset", in the case of resistive memory (ReRAM) or phase-change memory (PCRAM) types, are commonly used to indicate writing a low or high resistance state, respectively, to the memory cell. Endurance is the number of times data can be written to an NVM cell before it begins to commit errors. Due to technology, NVMs typically have a small number of endurance cycles, whereas SRAMs and DRAMs can effectively change the memory state an unlimited number of times.

NVMs type memories are affected by cumulative exposure to cosmic radiation over time, including total ionizing dose (TID). The effects caused by a single transient impact of energetic particles, known as single event effects (SEE), are the result/impact of the memory exposure to cosmic radiation.

Total ionizing dose TIDs modify the state of charge storage elements by altering the charge levels stored in the cell. All modern NVM technologies require CMOS control circuits, which are subject to threshold voltage shifts and sub-threshold leakage paths due to TID, which can cause read and write circuits to malfunction. More details about TID effects in electronics can be found in [2-4,9,11].

The displacement damage is caused by charged particles interacting with the electronic component structure and can also constantly modify the atomic structure. In such a case, some of the atoms that "constitute" one bit are delocalized, which can cause permanent memory lock or lack of functionality. It is often characterized by the flux of particles per unit area of the electronic component, presented as ion/cm^2 counts. In some cases atom delocalizations are also used to quantify deterioration. In NVMs most types of SEU are observed due to impact with heavy ions or high energy charged particles. Some of the usual events include non-permanent or soft errors known as single event errors (SEU), and also include single-bit errors (SBU) and multi-bit errors (MBU). One SBU event in an NVM memory cell refers to a change of state of a single bit due to a transient impact of a particle, usually due to charge accumulation, but in some cases it is possible for a charged particle to disturb the state of several bits in the NVM cell, in which case a MBU error occurs.

A single-event functional interrupt appears when the functionality of the memory controller circuitry, such as a microcontroller controlling the sequence of read and write operations, is affected by the impact of these particles. Table 1 shows the effects of TID and SEE on memories of different NVM memory types and their tolerance to cosmic radiation. [2].

Memories that are sensitive to relatively low radiation doses, are affected by the direct interaction of ionizing radiation with the stored charge. TID can cause bit-level perturbations at 10-50 krad (in Si semiconductor) and is largely unaffected by scaling. As multi-level cells and three-level cells (which store three bits per cell) become more common in scaled devices, these advanced cells are increasingly vulnerable to TID- and SEU-induced errors. Single-event disruptions easily occur in floating cells at Linear Energy Transfer (LET) values below 10 MeV*cm^2/mg. Floating-gate memory becomes more susceptible to bit perturbations with scaling as the stored charge for the expected state decreases. In contrast, advanced CTM-type memory is much more resistant, capable of withstanding TID levels between 300-500 krad (Si), with effective cross-sections for perturbation starting at a LET of approximately 20 MeV*cm^2/mg.

Taking into account the above, the reference radiation sensors are proposed in order to investigate the properties of the intelligent radiation sensor. Therefore, the properties and characteristics of two types of reference radiation sensors (RadFET and PIN diode array) are presented.

RadFET dosimetry. For a calibrated device to measure the accumulated radiation dose it was decided to use RadFET as the radiation dose sensing element. The most important advantages of RadFET-based dosimetry are [12,13]:

- sensor power can be completely switched off during irradiation (no power consumption and increased reliability); integrated measurement (particularly important for small doses);
- on-line, non-destructive reading and small size, on the other hand it has important drawbacks: low sensitivity at low radiation doses - requires sophisticated measurement setup and requires temperature compensation.

As a result of analyzing various satellite missions, we decided to take as a basis a sensor based on the RADFet effect, which can be read with time interval between readings can range from seconds to some days. The RadFET sensor (Reader Circuit - RC) designed circuit to read radiation value is presented in Figure 2.

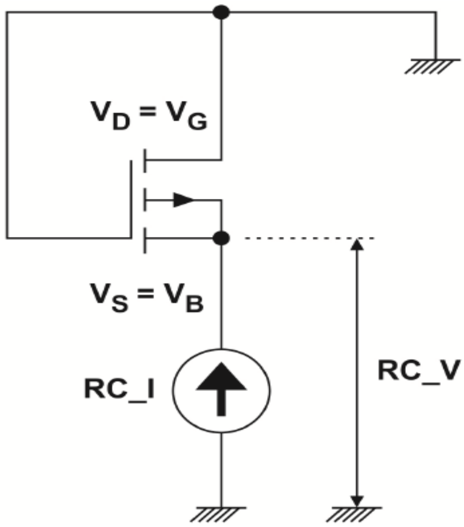

Figure 2. RadFET current measurement principle dependent on accumulated radiation dose [12,13].

The accumulated radiation dose is reflected by the readout current (RC_I) from the RADFET. But the current is measured indirectly, by measuring the source voltage (RC_V) - this voltage is called the "RC threshold voltage". For each RadFET element, there is the individual current-voltage (I-V) curve for the un-irradiated device, shown in Figure 3. In the given case the RC_I value was set above 10 μA for best temperature compensation.

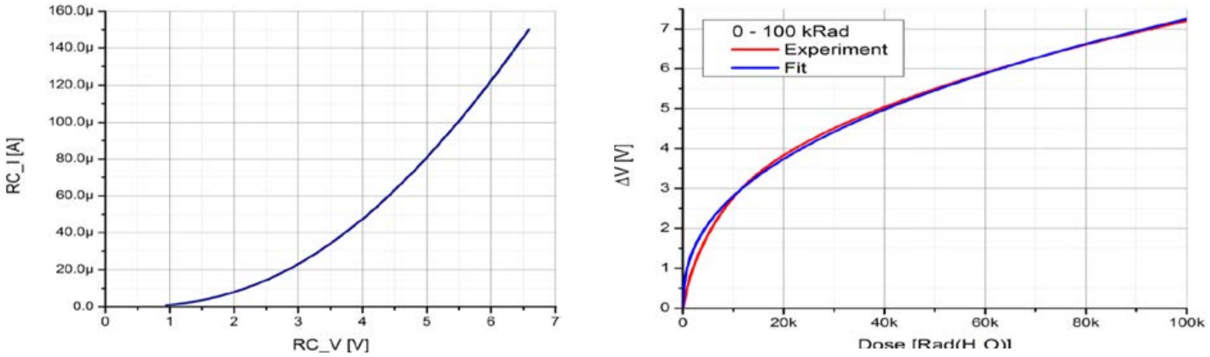

a) b)

Figure 3. RadFET characteristics: a) Pre-irradiation (I-V) curve measured at temperature 15 °C, b) curve of calibration during irradiation at normal temperature with gamma (Co-60) radiation source, dose rate ~50 Gy/h (5 krad/h) [12,13].

PIN-type diodes dosimetry. A positive-intrinsic-negative (PIN) diode has three layers, including an intrinsic layer sandwiched between the N- and P-type semiconductor crystal layers, with the specificity that the N-type layer is created when a pentavalent impurity is coated in the semiconductor region. In the P-type layer, a trivalent impurity is formed in the semiconductor region. The intermediate layer, called intrinsic, comprises an undoped semiconductor. The highly resistive intrinsic layer is positioned between the P and N regions and this intrinsic layer generates a strong electric field due to the movement of electrons and holes, causing the electric field to be directed from the N region to the P region. The strong electric field allows the diode to respond to small signals. The operation of a PIN diode is determined by the structure of its three-layer semiconductor structure, which consists of a p-type layer, an intrinsic (undoped or lightly doped) layer, and an n-type (negative) layer. The intrinsic layer, which is crucial for its function, behaves as a variable resistor when a voltage is applied. Radiation affects the PIN diode by generating uniformly distributed electron-hole (e-h) pairs within the diode. At high dose rates, the separation of these charges reduces the internal electric field and results in prolonged storage of excess carriers [1].

After analyzing the characteristics of PIN-diode sensors, the AL53 was chosen due to its solid state sensor performance and ultra low power requirements, making it an ideal option for both cutting-edge designs and retrofitting existing systems [14]. This AL53 radiation sensor features a custom designed PIN diode and to prevent sensitivity to light is coated with a thin aluminum film. The sensor diagram includes an integrated pulse discriminator with a temperature compensating threshold level, providing a TTL level output signal (Figure 4a). The AL53 radiation sensor is capable of detecting alpha and beta particles, as well as gamma rays.

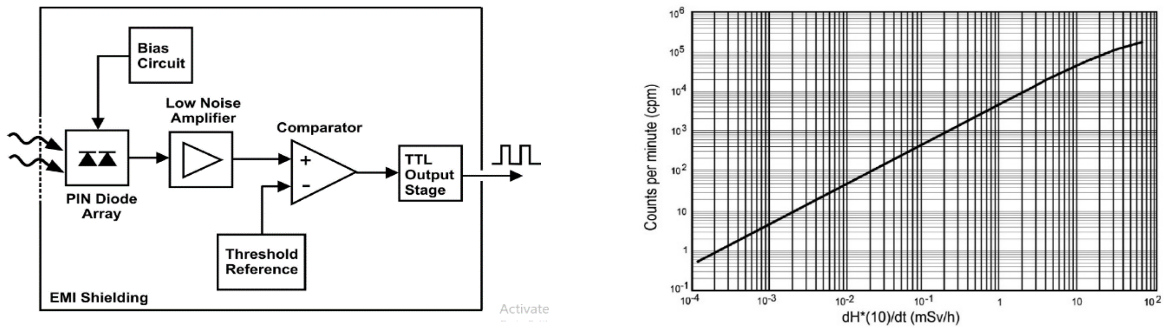

a) b)

Figure 4. AL53 PIN-diode [14]: a) Functional block diagram; b) curve of calibration during irradiation at normal at dH*(10)/dt - radiation dose rate for Cs-137 and Co-60 (mSv/h).

It should be noted an important side of these radiation sensors (RADFet and PIN-Diode) is that the former measures the cumulative dose, and the latter measures the current value of space radiation. These data we believe will be very useful for training of Artificial Neural Network.

Preliminary results

A preliminary FPGA design aimed at detecting SEUs and targeted at the AMD (Xilinx) UltraScale+ AU25P device is presented in [10]. It employs 100 blocks of SRAM (BRAMs) with a capacity of 36 Kb each, populated with a deterministic pattern of 1s and 0s that act as SEU detectors. Each such detector once triggered scans its memory content and can report and correct the encountered errors. The correct operation of the logic is insured by the TMR for all flip-flops (FFs) with separate replicas of the clock signal. The targeted AMD FPGA device was chosen based on its relatively low cost, available resources relative to the size and the implementation technology (i.e. the newest/smallest process for an FPGA-only AMD device – 16 nm). In [10] the design was analyzed regarding power consumption and real-time SEU detection capabilities. It was determined that a high clock signal frequency is unnecessary.

In the current work we analyze the same design but implemented on several other similar (in terms of resources, package footprint size and price) AMD FPGAs including one from the previous generation (using a 28 nm process) that is cheaper than the one used in

[10] while having comparable resources. The resources, package footprint size, resources and price for 10 devices are detailed in Table 2. The Look-Up Tables (LUTs) are all 6-bit, Ultra RAMs (URAMs) are block of SRAM 4K × 72 bits each (i.e. 288 Kb = 8 times larger than one BRAM) while each Digital Signal Processing (DSP) slice has a dedicated 25×18 bit two's complement multiplier and a 48-bit accumulator. The older XC7A200T device is potentially the most compact (i.e. 19×19 mm), and contains 65 more BRAMs than the AU25P device used in [10] while containing slightly less FFs and LUTs. However, it has significantly less DSPs that can be employed for the AI model.

Table 2

Comparative analysis of similar AMD FPGAs (in terms of resources, package footprint size and price)

Family	Device	Size	FFs	LUTs	BRAMs	URAM	DSPs	Approx. Price (x10)
Artix-7	**XC7A200T**	19×19 23×23 27×27	269200	134600	365	0	740	$3900
Artix UltraScale+	**AU20P**	23×23	218000	109000	200	0	900	$5900
Artix UltraScale+	**AU25P**	23×23	282000	141000	300	0	1200	$7000
Kintex UltraScale+	**KU3P**	23×23	325440	162720	360	48	1368	$22900
Kintex UltraScale+	**KU5P**	23×23	433920	216960	480	64	1824	$31000

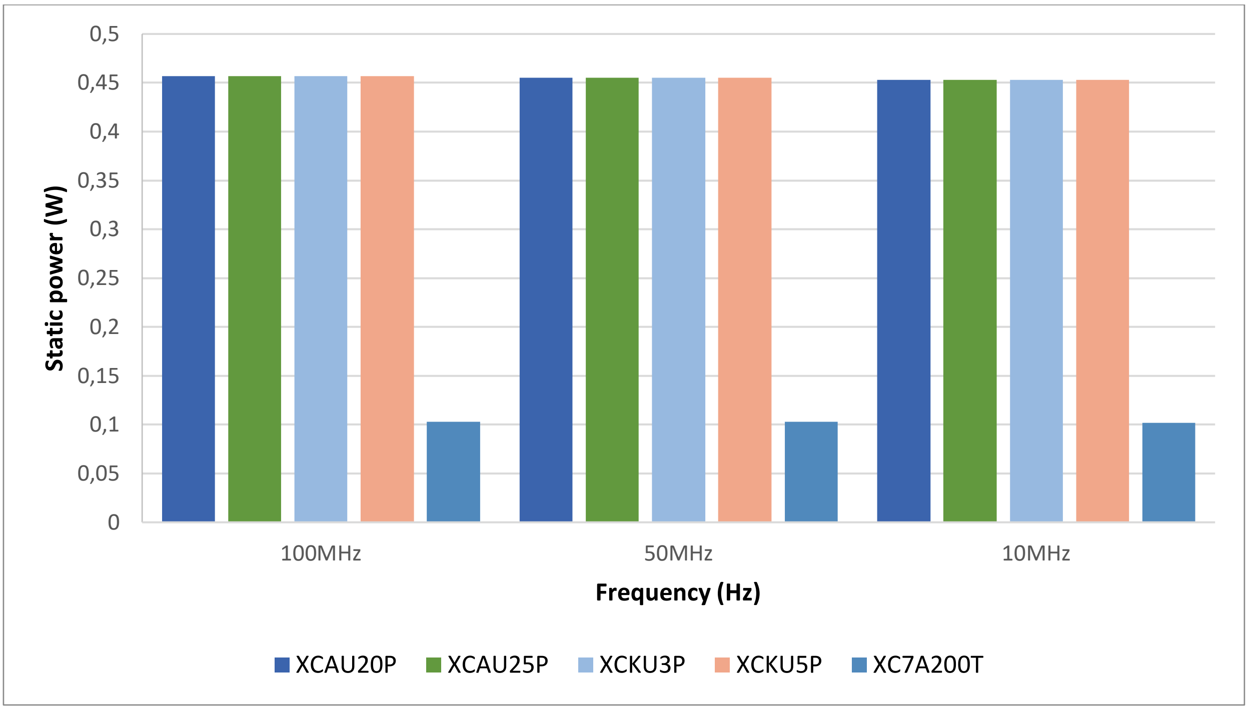

Figure 5. The static power consumptions for the five considered AMD FPGAs.

Like in [10] we targeted 3 frequencies for the clock signals: 10, 50 and 100 MHz. The static, dynamic and total (i.e. static plus dynamic) power consumptions are listed in Figures 5, 6 and 7, respectively. Even though the same tool is used (i.e. AMD Vivado 2024.1) with the same constraints, design and settings, the much lower static power draw of the older XC7A200T device makes it the most energy-efficient device from the selected ones. This trend remains when estimating the power consumption using the signals toggling rates extracted from simulations.

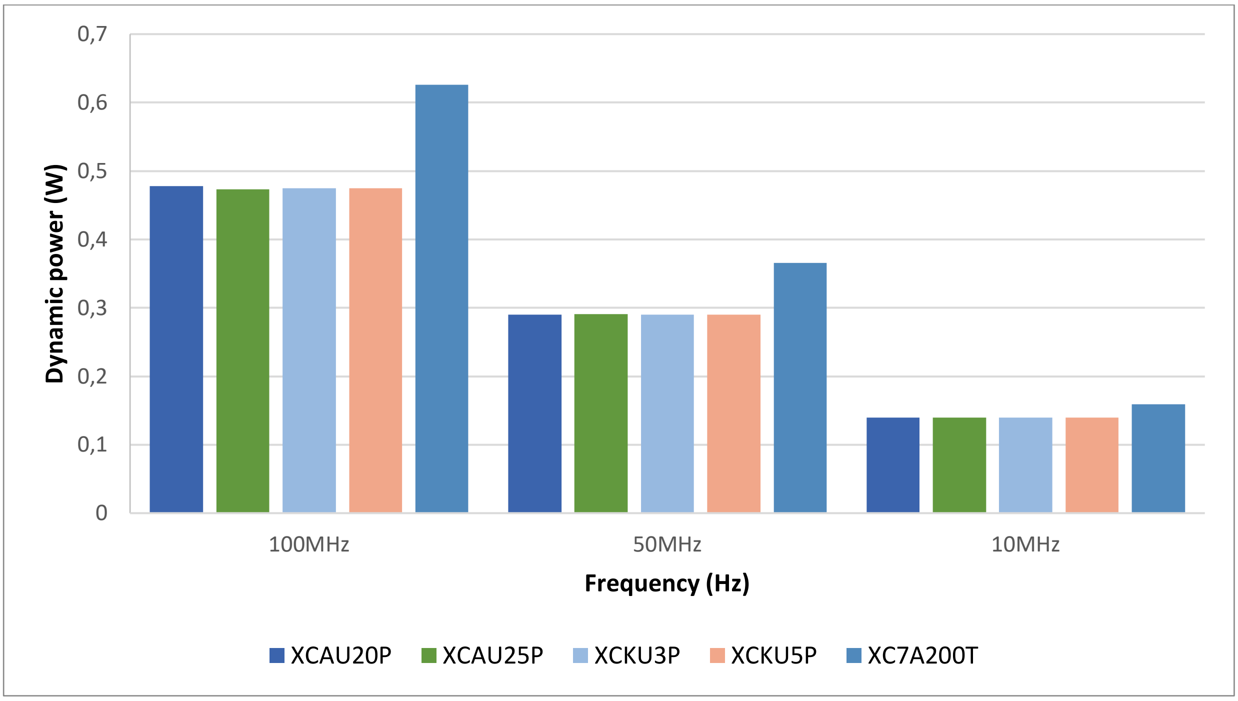

Figure 6. The dynamic power consumptions for the five considered AMD FPGAs.

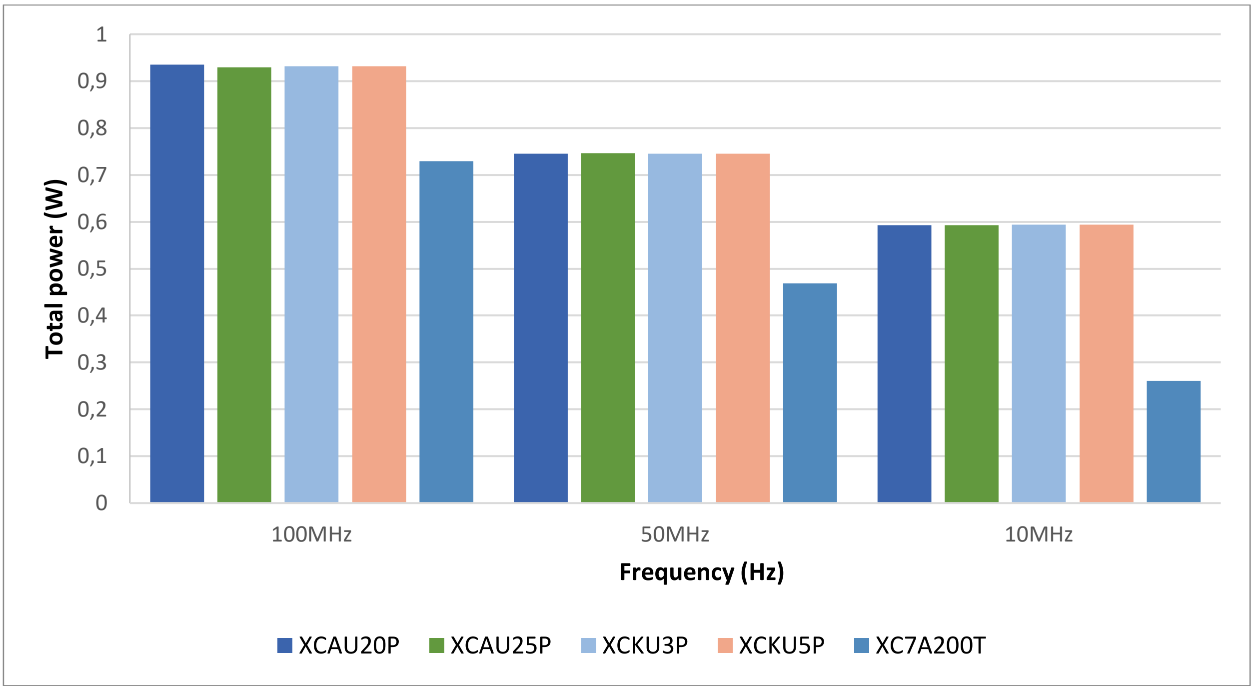

Figure 7. The total power consumptions for the five considered AMD FPGAs.

In this preliminary analysis for choosing the FPGA device we also consider the sensibility of the device to nuclear radiation. In [15] the determined BRAM cross-sections for the Artix-7 and the UltraScale+ FPGA families are 6.32×10^{-15} cm^2/bit and 9.82×10^{-16} cm^2/bit. These amounts are determined from LANSCE (Los Alamos Neutron Science Center) beam testing. The older XC7A200T device is one order of magniture more susceptiple to nuclear radiation compared to the UltraScale+ devices which is advantageous in our case.

Considering all these characteristics, the AMD Artix-7 XC7A200T FPGA device was selected, which is the most energy efficient among the selected ones, and this trend is maintained when estimating the power consumption using the switching rates of the signals extracted from the simulations with back-to-back scanning (see Figures 5, 6 and 7).

Conclusion

In this paper, a study of the types of cosmic radiation and its effects on electronic circuits has been carried out. Particular attention has been paid to the methods of measuring cosmic radiation in order to design a smart sensor. The architecture of the satellite module with the smart radiation sensor based on an FPGA circuits was proposed, which includes radiation sensing elements, arrays of different types of electronic memories (on semiconductors), both inside and outside the circuit, which wll classify and analyze in real time the fault patterns induced by cosmic radiation and predict the state of the electronic systems embedded in satellites.

In order to exclude the influence of space radiation on the FPGA core it is proposed to realize acquisition, processing and communication procedures using TMR. The FPGA device was selected, which is the most energy efficient from the considered ones energy efficient The FPGA device was selected based on its estimated power draw, avaible resources, total cross section to maximize its susceptibly to radiation and price.

Acknowledgment

This work was funded by the Romanian Ministry of Research, Innovation and Digitalization, project PN-IV-P8-8.3-ROMD-2023-0068 entitled ”Artificial Intelligence-enabled Hardware Cosmic Radiation Sensor for Space Applications (AICoRS)”, contract no. 2ROMD/01.06.2024.

Conflicts of Interest: The author declares no conflict of interest.

Reference

1. Knoll, G.F. *Radiation Detection and Measurement*. John Wiley&Sons, NJ, SUA, 2000, p. 816.
2. Marinella, M. J. Radiation Effects in Advanced and Emerging Nonvolatile Memories. In: *IEEE Transactions on Nuclear Science* 2021, 68(5), pp. 28.
3. Verrelli, E.; Tsoukalas, D. Radiation Hardness of Flash and Nanoparticle Memories. *InTech* 2011, pp. 210-240.
4. Taggart, J.L. Ionizing radiation effects on nonvolatile memory properties of programmable metallization cells. *IEEE Transactions on Nuclear Science* 2014, 61 (6), pp. 2985–2990.
5. Wirthlin, M. High-Reliability FPGA-Based Systems: Space, High-Energy Physics, and Beyond. *Proceedings of the IEEE*, 2015, 103(3), pp. 379–389.
6. Wu, R.X.; Guo, J.; Du, J.; Li, J. Accelerating neural network inference on fpga-based platforms—a survey. *Electronics*, 2021, 10(9), 1025.
7. AMD. XQR Space-Grade Kintex™ UltraScale™ and Space Heritage. 2023, Available online: https://www.xilinx.com/publications/solution-briefs/xilinx-space-solution-brief.pdf (accessed on 06.06.2024).
8. Parkes, S. SpaceWire User's Guide. Available online: https://www.star-dundee.com/wp-content/star_uploads/general/SpaceWire-Users-Guide.pdf (accessed on 07.06.2024).
9. Popa, S.; Martoiu, S.; Ivanovici, M. Study of the ATLAS new small wheel read-out controller ASIC in a neutron irradiation environment. Journal of Instrumentation 2020, 15(10), P10023.

10. Popa, S.; Kazak, A.; Dinu, A.; Ivanovici, M.; Secrieru, N.; Carbune, V.; Melnic, V. Architecture and Design Choices for an AI-enabled FPGA-based Cosmic Radiation Sensor. In: The paper of the ISTEC-2024 16th International Symposium on Electronics and Telecommunications (ISETC), Timisoara, November 6-7, 2024, p. 4.
11. Gerardin, S.; Paccagnella, A. Present and future non-volatile memories for space. IEEE Trans. Nuclear Science 2010, 57(6), pp. 3016–3039.
12. Varadis. Radfet, radiation detection sensors and dosimetry systems, 2024. Available online: https://www.varadis.com/products/ (accessed on 06.07.2024).
13. Bostan, V.; Bostan, I.; Ilco, V.; Melnic, V.; Martîniuc, A.; Vărzaru, V.; Secrieru, N.; Guţu, M.; Verjbiţki, V.; Magariu, N.; Lupan, O. KiboCUBE Program: the challenges and experience of the Technical University of Moldova on the development of nanosatellites. Bons Offices, Chisinau, RM, 2022, 259 p. ISBN 978-9975-166-65-2.
14. Teviso. Alpha Particle Sensor AL53. 2023. Available online: https://www.teviso.com/file/pdf/al53-data-specification.pdf (accessed on 07.06.2024).
15. AMD. Device Reliability Report. 2024. Available online: https://docs.amd.com/r/en-US/ug116/The-Reliability-Program UG116 (v10.18), (accessed on 07.06.2024).

Citation: Secrieru, N.; Cărbune, V.; Zadorojneac, T.; Melnic, V.; Bertescu A.; Ivanovici, M.; Popa, Ș.; Kazak, A. Architecture of the space radiation sensor satellite module based on artificial intelligence. *Journal of Engineering Science* 2024, XXXI (4), pp. 73-83. https://doi.org/10.52326/jes.utm.2024.31(3).01.

Publisher's Note: JES stays neutral with regard to jurisdictional claims in published maps and institutional affiliations.

Submission of manuscripts: jes@meridian.utm.md